

Supporting Information

An activity-based fluorescent probe and its application for
differentiating alkaline phosphatase activity in different cell lines

Yong He,^{a‡} Junli Yu,^{b‡} Xiangzi Hu,^{a‡} Shumei Huang,^a Lili Cai,^a Liu Yang,^{c,d}
Huatang Zhang,^{a*} Yin Jiang,^{a*} Yongguang Jia,^e Hongyan Sun^{c,d*}

^a School of Chemical Engineering and Light Industry, School of Biomedical and Pharmaceutical Sciences, Guangdong University of Technology, Guangzhou, Guangdong, 510006, China.

^b Department of Ultrasonography, The Sixth Affiliated Hospital of Sun Yat-sen University, Guangzhou, 510655, China

^c Department of Chemistry and Center of Super-Diamond and Advanced Films (COSDAF), City University of Hong Kong, 83 Tat Chee Avenue, Kowloon, Hong Kong, China.

^d Chengdu Research Institute, City University of Hong Kong, Chengdu, 610200, China.

^e National Engineering Research Center for Tissue Restoration and Reconstruction, South China University of Technology, Guangzhou 510006, China

*Corresponding author: htzhang@gdut.edu.cn, Tel./fax: 86-20-39322230

yjiang@gdut.edu.cn, Tel./fax: 86-20-39322230

hongysun@cityu.edu.hk, Tel./fax: 852-34429537

‡ These authors have the equivalent contribution to this work.

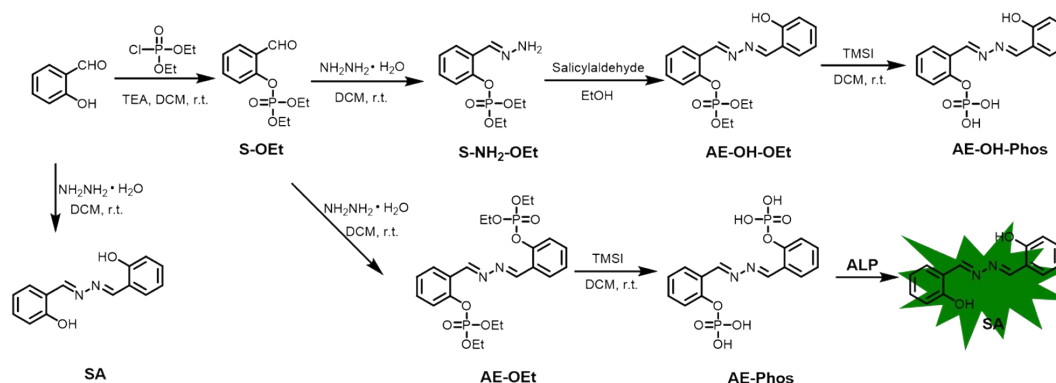
1. Experiment

1.1 Materials and instruments

All chemicals were purchased from commercial companies with analytical grade and used directly without further purification unless otherwise specified. (Trifluoromethyl)trimethylsilane was bought from Meryer. Triethylamine, salicylaldehyde, hydrazine hydrate, diethyl chlorophosphate and dry solvent (DCM, methanol, ethanol) were obtained from Adamas-beta®. Dulbecco's modified Eagle's medium (DMEM), Tris buffer, fetal bovine serum (FBS), trypsin-EDTA and penicillin/streptomycin were purchased from Invitrogen. All reactions that utilize air- or moisture sensitive reagents were performed in dried glassware under dry Ar atmosphere. Milli-Q water was used in all experiments. The progress of the reaction was monitored by thin-layer chromatography. ¹H NMR, ¹³C NMR and ³¹P NMR spectra were taken on a Bruker 400 MHz NMR spectrometer. UV-vis absorption spectra were obtained on Shimadzu UV-3600 Spectrophotometer. Fluorescence spectra were acquired with FluoroMax-4 fluorescence photometer. Fluorescence images were captured using ZEISS LSM 800 with Airscan Confocal Laser Scanning Microscope.

1.2 Synthesis

AE-Phos was synthesized according to the procedure illustrated in Scheme S1. The uncaged product (SA) and the intermediate product (AE-OH-Phos) were also synthesized to examine the dephosphorylation mechanism of ALP.



Scheme S1 Synthesis route of SA, AE-OH-Phos and **AE-Phos** and reaction mechanism with ALP.

1.2.1 Synthesis of SA

Under argon atmosphere, salicylaldehyde (500 mg, 4.1 mmol) was dissolved in dry DCM (10 mL). Hydrazine hydrate (103 mg, 2.1 mmol) was then added to the solution. The reaction solution was stirred for 3 hours and monitored by TLC. After the reaction completed, the reaction solution was washed with saturated brine solution and dried with Na_2SO_4 . The organic solvent was concentrated under vacuum, and the crude product was purified by column chromatography with silica gel (PE/EA=3/1, v/v) to give the pure compound SA as a yellow solid (428 mg, 87%). ^1H NMR (400 MHz, $\text{d}^6\text{-DMSO}$) δ : 11.12 (s, 2H), 9.01 (s, 2H), 7.70 (dd, $J = 7.78, 1.39$ Hz, 2H), 7.41 (m, 2H), 6.99 (d, $J = 7.94$ Hz), 6.98 (m, 1H).

1.2.2 Synthesis of S-OEt

Salicylaldehyde (500 mg, 4.1 mmol) and triethylamine (680 μL) were dissolved in dry DCM (20 mL) under argon atmosphere. Diethyl chlorophosphite (836 mg, 4.8 mmol) were then added to the solution. The reaction mixture was stirred overnight at room temperature and monitored by TLC. When the reaction was complete, DCM was added to dissolve the white precipitate. The DCM layer was washed with saturated brine solution and dried with Na_2SO_4 . After the organic solvent was concentrated under vacuum, the crude product was purified by column chromatography with silica gel (PE/DCM=1/1, v/v) to give the pure product S-OEt as a yellow oil (900 mg, 84%). ^1H NMR (400 MHz, CDCl_3) δ : 10.40 (d, $J = 0.56$ Hz, 1H), 7.89 (m, 1H), 7.59 (m, 1H), 7.46 (d, $J = 8.34$ Hz, 1H), 7.29 (m, 1H), 4.25 (m, 4H), 1.35 (dt, $J = 7.08, 7.08, 1.05$ Hz, 6H). ^{31}P NMR (CDCl_3 , 162 MHz) δ : -6.66 Hz.

1.2.3 Synthesis of S-NH₂-OEt

S-OEt (440 mg, 1.7 mmol) was dissolved in dry ethanol and slowly added to the ethanol solution containing hydrazine hydrate (175 mg, 3.5 mmol). The solution was stirred for 3 hours at room temperature. Then the solvent was concentrated under vacuum and the residue was purified by column chromatography with silica gel (PE/EA=2/1, v/v) to give compound S-NH₂-OEt

as a yellow solid (370 mg, 80%). ^1H NMR (400 MHz, CDCl_3) δ : 10.372 (d, $J = 0.65$ Hz, 1H), 7.85 (m, 1H), 7.56 (m, 1H), 7.43 (d, $J = 8.33$ Hz, 1H), 7.26 (m, 1H), 4.21 (m, 4H), 1.32 (dt, $J = 7.07, 7.07, 1.06$ Hz, 6H). ^{13}C NMR (100 MHz, $\text{d}^6\text{-DMSO}$) δ : 156.42, 149.96, 149.93, 133.11, 127.53, 125.66, 124.83, 120.92, 64.73, 15.86. ^{31}P NMR ($\text{d}^6\text{-DMSO}$, 162 MHz) δ : -6.38 Hz.

1.2.4 Synthesis of AE-OH-OEt

S-NH₂-OEt (300 mg, 1.1 mmol) and salicylaldehyde (269 mg, 2.2 mmol) were dissolved in dry ethanol. The reaction mixture was stirred overnight at room temperature and monitored by TLC. The solvent was then concentrated under vacuum, and the residue was purified by column chromatography with silica gel (pure DCM) to give compound AE-OH-OEt as a yellow solid (340 mg, 82%). ^1H NMR (400 MHz, $\text{d}^6\text{-DMSO}$) δ : 11.12 (s, 1H), 8.98 (s, 1H), 8.88 (s, 1H), 8.01 (d, $J = 7.75$ Hz, 1H), 7.72 (dd, $J = 7.64, 1.64$ Hz, 1H), 7.60 (m, 1H), 7.41 (m, 1H), 7.38 (s, 1H), 7.36 (m, 1H), 6.98 (d, $J = 1.49$ Hz, 1H), 6.95 (m, 1H), 4.19 (m, 4H), 1.26 (td, $J = 7.04, 7.04, 0.96$ Hz, 6H). ^{13}C NMR (100 MHz, $\text{d}^6\text{-DMSO}$) δ : 163.22, 158.66, 156.27, 149.93, 133.28, 133.08, 130.85, 127.38, 125.66, 124.86, 120.98, 119.57, 118.19, 116.48, 64.72, 15.87. ^{31}P NMR ($\text{d}^6\text{-DMSO}$, 162 MHz) δ : -6.41 Hz.

1.2.5 Synthesis of AE-OH-Phos

Under argon atmosphere, AE-OH-OEt (100 mg, 0.27 mmol) was dissolved in dry DCM (10 mL). Trimethylsilyl iodide (540 mg, 2.7 mmol) was then added dropwise to the solution. The reaction mixture was stirred overnight at room temperature and monitored by TLC. When the reaction was complete, the intermediate product was obtained by removing the organic solvent in vacuum. The intermediate product was dissolved in methanol (10 ml), and the solution was stirred overnight at room temperature under argon atmosphere. A yellow solid was observed to precipitate out. After the reaction was completed, EA was added to wash the solid, and filtered to obtain compound AE-OH-Phos as a black solid (53 mg, 61%). ^1H NMR (400 MHz, $\text{d}^6\text{-DMSO}$) δ : 8.98 (d, $J = 9.88$ Hz, 1H), 8.93 (d, $J = 2.51$ Hz, 1H), 8.07 (t, $J = 7.27, 7.27$ Hz, 1H), 7.70 (dt, $J =$

8.08, 7.89, 1.42 Hz, 1H), 7.53 (m, 1H), 7.41 (d, $J = 1.43$ Hz, 1H), 7.38 (m, 1H), 7.27 (d, $J = 5.66$ Hz, 1H), 6.97 (d, $J = 7.94$ Hz, 1H), 6.94 (m, 1H). ^{13}C NMR (100 MHz, $\text{d}^6\text{-DMSO}$) δ : 163.17, 162.78, 158.66, 157.09, 133.23, 132.74, 131.04, 103.84, 126.69, 124.60, 121.40, 119.61, 118.18, 116.51. ^{31}P NMR ($\text{d}^6\text{-DMSO}$, 162 MHz) δ : -6.15 Hz.

1.2.6 Synthesis of AE-OEt

S-OEt (500 mg, 1.94 mmol) was dissolved in dry DCM (5 mL) under argon atmosphere. Hydrazine hydrate (50 mg, 1 mmol) was then added to the solution. The solution was stirred for 3 hours and monitored by TLC. After the reaction was completed, the reaction solution was washed with saturated brine solution and dried with Na_2SO_4 . The organic solvent was subsequently concentrated under vacuum, and the crude product was purified by column chromatography with silica gel (pure DCM) to give the pure product AE-OEt as a yellow solid (400 mg, 86%). ^1H NMR (400 MHz, $\text{d}^6\text{-DMSO}$) δ : 8.87 (s, 2H), 8.11 (d, $J = 7.75$ Hz, 2H), 7.61 (m, 2H), 7.40 (d, $J = 8.48$ Hz, 2H), 7.37 (m, 2H), 4.19 (m, 8H), 1.27 (dt, $J = 7.04, 7.04, 0.88$ Hz, 12H). ^{13}C NMR (100 MHz, $\text{d}^6\text{-DMSO}$) δ : 156.42, 149.93, 133.11, 127.54, 125.66, 124.94, 120.93, 64.73, 15.87. ^{31}P NMR ($\text{d}^6\text{-DMSO}$, 162 MHz) δ : -6.38 Hz.

1.2.7 Synthesis of AE-Phos

AE-OEt (256 mg, 0.5 mmol) was dissolved in dry DCM (10 mL) under argon atmosphere. Trimethylsilyl iodide (500 mg, 2.5 mmol) was then added dropwise and slowly to the solution. The reaction mixture was stirred overnight at room temperature and monitored by TLC. When the reaction was complete, the red viscous oil product was obtained by removing the organic solvent in vacuum. The red viscous oil product was then dissolved in methanol (10 mL) and stirred overnight at room temperature under argon atmosphere. When the reaction was complete, the solvent was removed and EA was added. The product was extracted with water from the EA, and the aqueous phase was retained. The water layer was subsequently dried by freeze-drying technology to obtain the final product AE-Phos (232 mg, 58%). ^1H NMR (400 MHz, $\text{d}^6\text{-DMSO}$) δ : 8.87

(s, 2H), 8.03 (d, $J = 7.69$ Hz, 2H), 7.50 (t, $J = 8.48, 8.48$ Hz, 2H), 7.38 (d, $J = 8.26$ Hz, 2H), 7.22 (t, $J = 7.53, 7.53$ Hz, 2H). ^{13}C NMR (100 MHz, $\text{d}^6\text{-DMSO}$) δ : 156.92, 152.26, 132.92, 127.08, 125.58, 124.67, 121.81. ^{31}P NMR ($\text{d}^6\text{-DMSO}$, 162 MHz) δ : -5.93 Hz.

1.3 General procedure for absorption and fluorescent measurement

AE-Phos was dissolved in an appropriate amount of DMSO to obtain 5 mM stock solution. ALP was diluted in Tris-HCl buffer (50 mM, pH 7.4) from 10,000 U/mL stock solution. Other biological analytes were prepared as 1 mM or 10 mM stock solutions or other appropriate concentrations in Tris buffer. All the measurements were taken under 37 °C in Tris buffer (50 mM, pH 7.4). The excitation wavelength was set at 356 nm. The emission wavelength was set in the range of 450 nm to 650 nm. The slit widths of excitation and emission wavelength were both set at 5 nm.

1.4 Kinetic experiment

All kinetic measurements were performed in Tris-HCl buffer (50 mM, pH 7.4) at 37 °C. Briefly, different concentrations of **AE-Phos** (0.5, 1, 1.5, 2.5, 3.5, 5, 10, 20 μM) were added into the ALP solution (100 U/L) in Tris buffer. The resulting fluorescence intensity was recorded at 536 nm every 20 seconds for 2 min. The fluorescence standard curve of SA was used to calculate the reaction rate under the same conditions. The parameters of the enzyme reaction kinetics, Michaelis-Menten constant (K_m), maximum rate (V_{max}) and catalytic rate constant (K_{cat}) were determined according to Michaelis-Menten equation, $V = V_{\text{max}}[S]/(K_m+[S])$. The results reported here are the average values of three independent experiments.

1.5 ALP assay imaging in different cell lines

Cells were seeded onto a glass-bottom confocal dish and cultured in DMEM supplemented with appropriate amount of antibiotic (penicillin and streptomycin) under 5% CO_2 at 37 °C and incubated for 24 h. Subsequently the cells were incubated with **AE-Phos** (5 μM) in DMEM for 2 h. They were then washed with DMEM and Tris buffer to remove the extracellularly distributed

probes and the reaction product in the medium. For the inhibition experiment, cells were pretreated with Na_3VO_4 (1 mM) for 20 min, incubated with **AE-Phos** (5 μM) at 37 °C for 2 h and then washed with the above procedure. Fluorescence imaging was then carried out using ZEISS LSM 800 with Airscan Confocal Laser Scanning Microscope with 40× oil objectives. Ex: 405 nm, Em: 500-600 nm.

2. Supplementary Figures

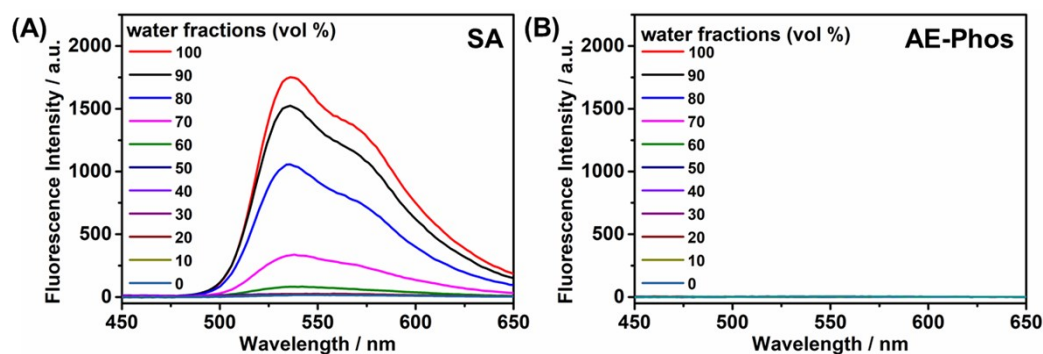


Fig. S1 Fluorescence spectra of SA (5 μM) (A) and AE-Phos (5 μM) (B) at different water fractions. Ex:365 nm.

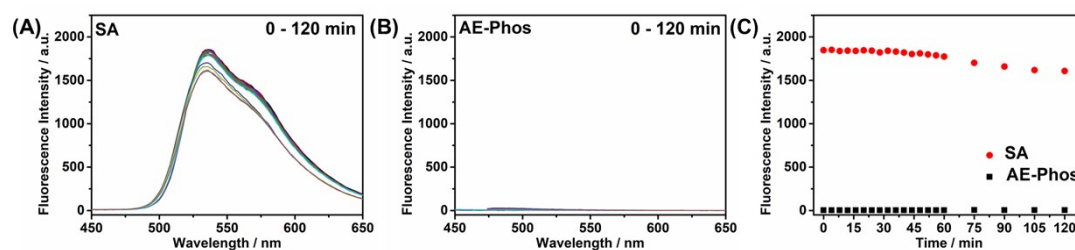


Fig. S2 Fluorescence spectra of SA (5 μM) (A) and AE-Phos (5 μM) (B) upon incubation in Tris buffer at 37 $^{\circ}\text{C}$ for 2 hours; (C) Fluorescence intensity of SA (5 μM) and AE-Phos (5 μM) at 536 nm at different incubation time.

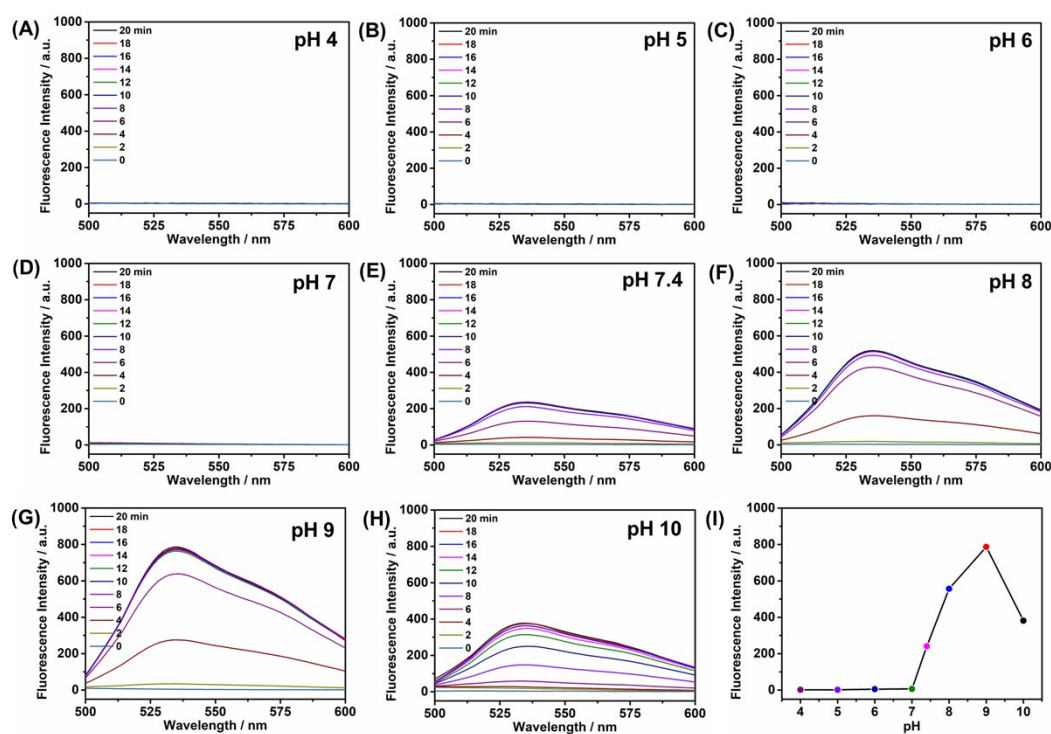


Fig. S3 Fluorescence spectra of AE-Phos (5 μM) toward ALP (100 U/L) in different pH Tris buffer at 37 $^{\circ}\text{C}$ for 20 min incubation. The fluorescence spectra were recorded every 2 min.

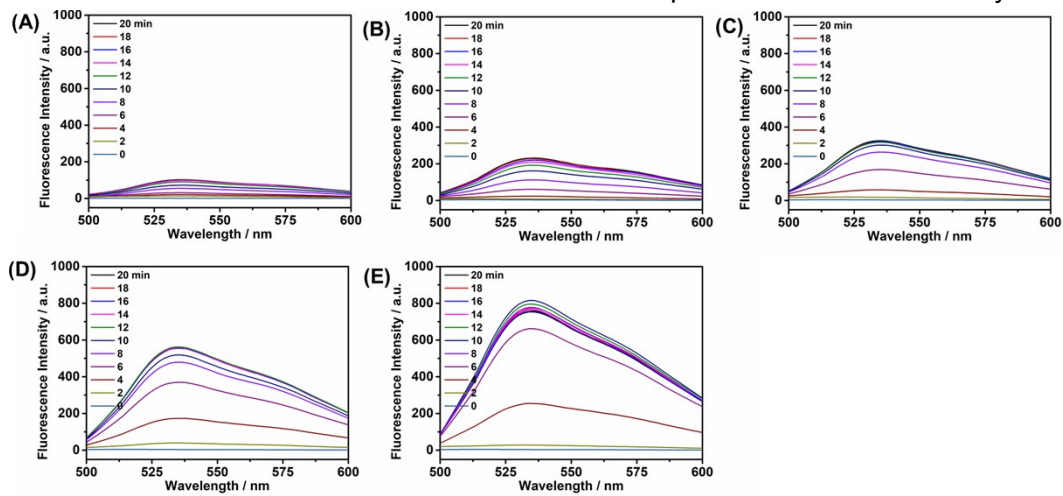


Fig. S4 Fluorescence spectra of AE-Phos (5 μM) toward different concentration of ALP in Tris buffer (pH 9.0, 50 mM) at 37 $^{\circ}\text{C}$. The fluorescence spectra were recorded every 2 min.

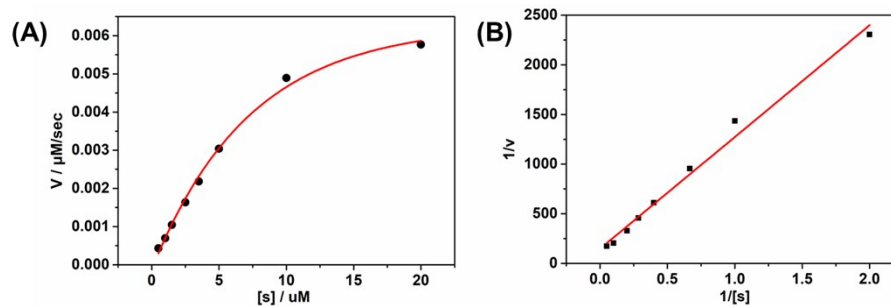


Fig. S5 (A) Michaelis-Menten plots of the initial velocity (v) of the hydrolysis of AE-Phos by ALP against the concentration of AE-Phos (S); (B) Plot of reciprocal initial velocity ($1/v$) against reciprocal substrate concentration ($1/s$).

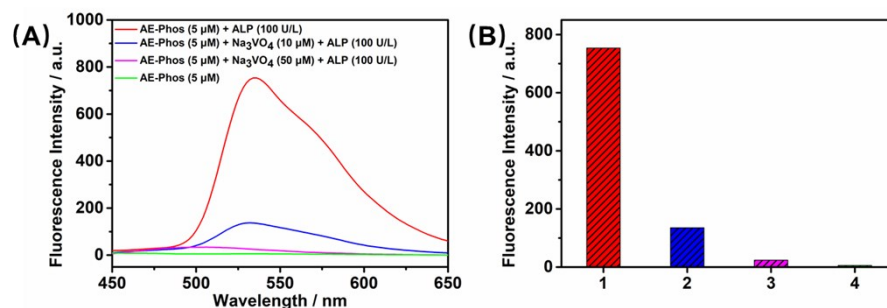


Fig. S6 (A) Fluorescence spectra of the inhibition study between AE-Phos (5 μM) and ALP (100 U/L) in the presence of different concentrations of Na_3VO_4 (0 μM , 10 μM , 50 μM); (B) Fluorescence intensity at 536 nm of AE-Phos (5 μM) and ALP (100 U/L) with different concentration of Na_3VO_4 after 30 min incubation in Tris buffer (pH 9.0, 10 mM) at 37 $^{\circ}\text{C}$.

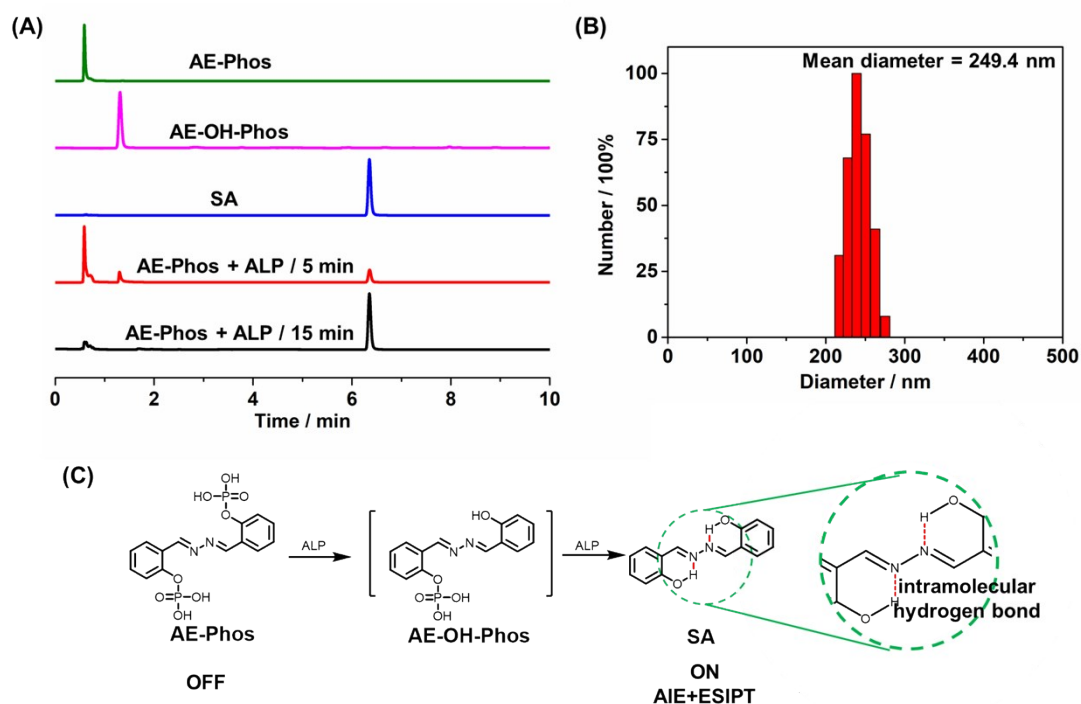


Fig. S7 (A) Reversed-phase UPLC chromatograms of the solution of various substrates in Tris buffer (pH 9.0, 50 mM). The absorption wavelength was recorded at 254 nm. $\text{H}_2\text{O}-\text{CH}_3\text{CN}$, from 90:10 to 10:90 in 10 min; flow rate: 0.2 mL/min; column: 2.1×50 mm; (B) DLS analysis of **AE-Phos** (5 μM) after incubation with ALP (100 U/L) in Tris buffer for 15 min at 37 $^{\circ}\text{C}$; (C) Proposed reaction mechanism of **AE-Phos** based on AIE and ES IPT.

Table S1 Comparison of AE-Phos and other ALP fluorescent probes.

Probe	$\lambda_{ex}/$ nm	$\lambda_{em}/$ nm	Stokes shift /nm	Fluorescence enhanced fold	Detection limit / U·L ⁻¹	Reaction time / min	Vmax / μ M·min ⁻¹	K _m / μ M	Ref.
TP-Phos Biomaterials 2017, 140, 220.	365	500	135	12-fold probe: 5 μ M ALP:10 U/L	0.30	25	4.38	8.56	[S1]
DHXP ACS Appl. Mater. Interfaces 2017, 9, 6796	680	700	20	66-fold probe: 5 μ M ALP:100 U/L	0.07	30	/	21.2	[S2]
P-Cy-Gd J. Am. Chem. Soc. 2019, 141, 10331	680	710	30	70-fold Probe: 5 μ M ALP:100 U/L	0.017	30	1.05	13.14	[S3]
Probe J. Mater. Chem. B 2015, 3, 1042	425	554	129	17-fold probe :5 μ M ALP:75 U/L	0.38	20	1.506	22.51	[S4]
Probe 1 Chem. Commun. 2011,47, 9825	460	529	69	90-fold probe:10 μ M ALP :350 nM	/	30	/	19.2	[S5]
NALP Talanta 2017, 175, 421	680	706	26	57-fold probe: 1 μ M ALP:40 U/L	0.28	30	4.41	52.45	[S6]
DHP Dyes Pigm. 2018, 159, 584	570	615	45	17-fold probe:10 μ M ALP :10 U/L	0.031	30	/	/	[S7]
CyP Anal. Chem. 2017, 89, 6854	690	738	48	10-fold probe:10 μ M ALP:2 U/mL	3	20	0.693	9.32	[S8]
QcyP Sens. Actuators B Chem. 2018, 265, 565	575	685	115	/	0.31	30	/	9.75	[S9]
APT Anal. Chim. Acta 2020, 1094, 113	450	650	200	14-fold probe:10 μ M ALP:100 U/L	0.89	10	0.108	1.64	[S10]
AE-Phos	356	536	180	240-fold probe:5 μ M ALP:100 U/L	0.012	10	0.408	7.66	This work

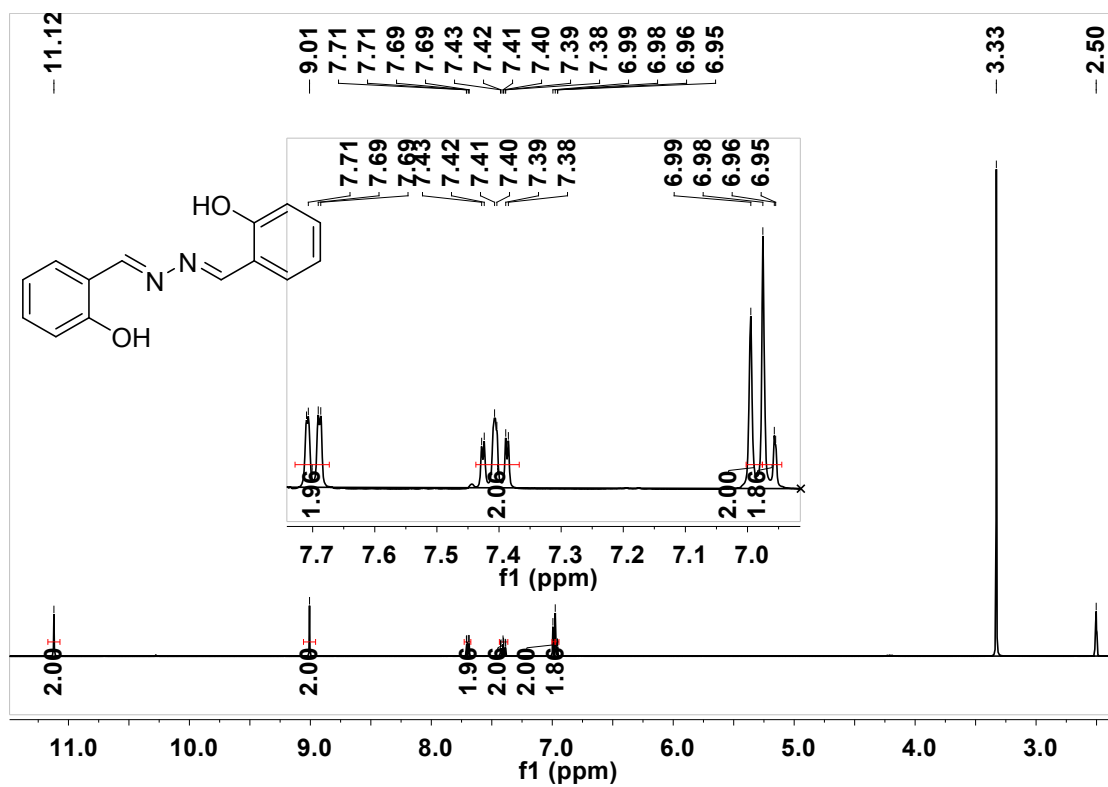


Fig. S8 ¹H NMR spectrum of compound SA (d⁶-DMSO).

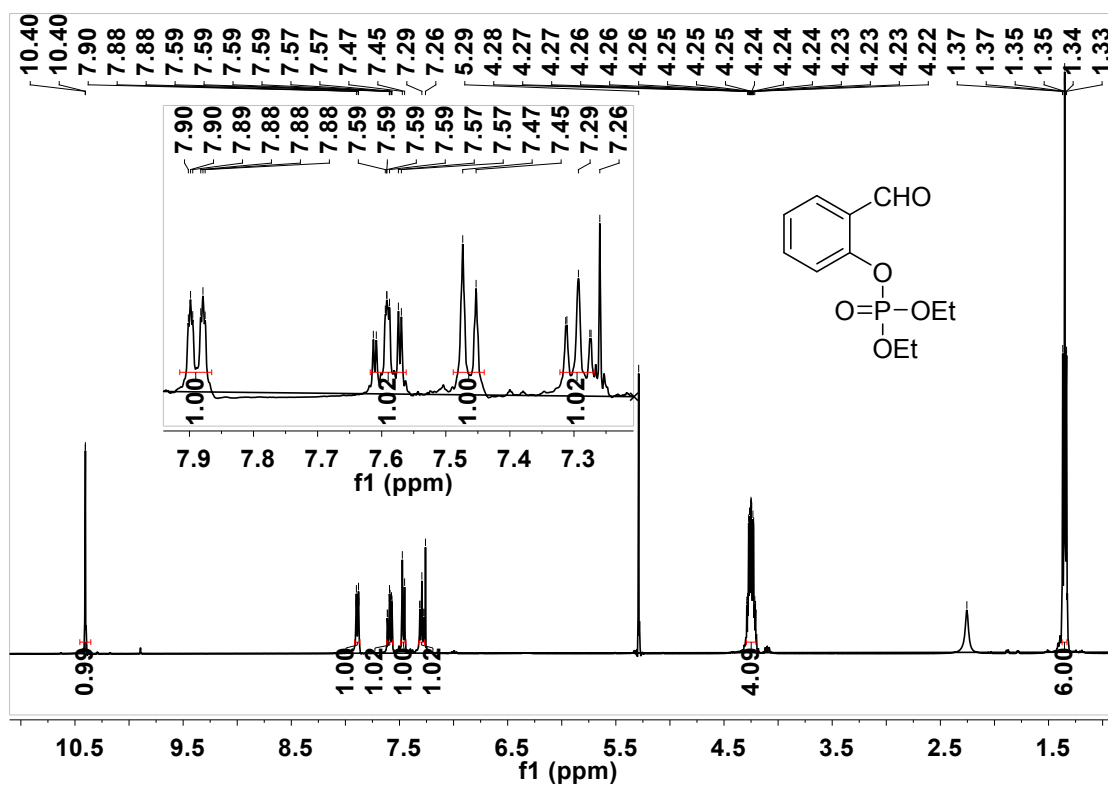


Fig. S9 ¹H NMR spectrum of compound S-OEt (CDCl₃)

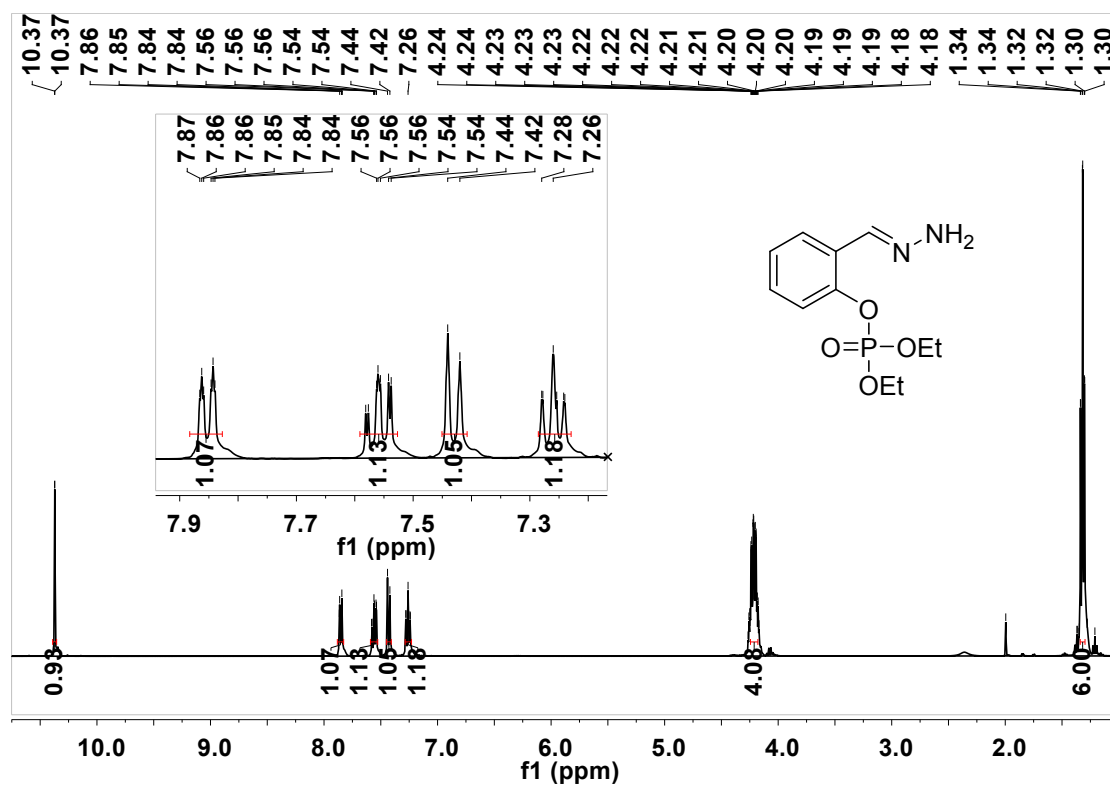


Fig. S10 ¹H NMR spectrum of compound S-NH₂-OEt (CDCl₃).

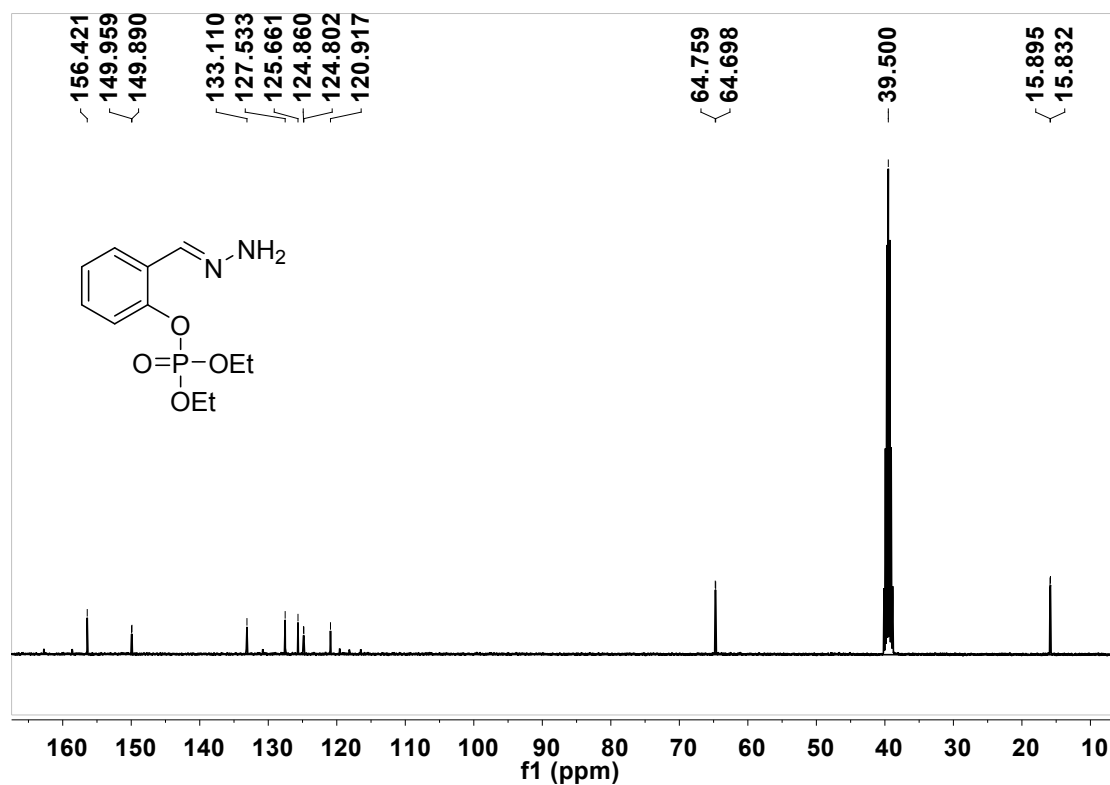


Fig. S11 ¹³C NMR spectrum of compound S-NH₂-OEt (d⁶-DMSO).

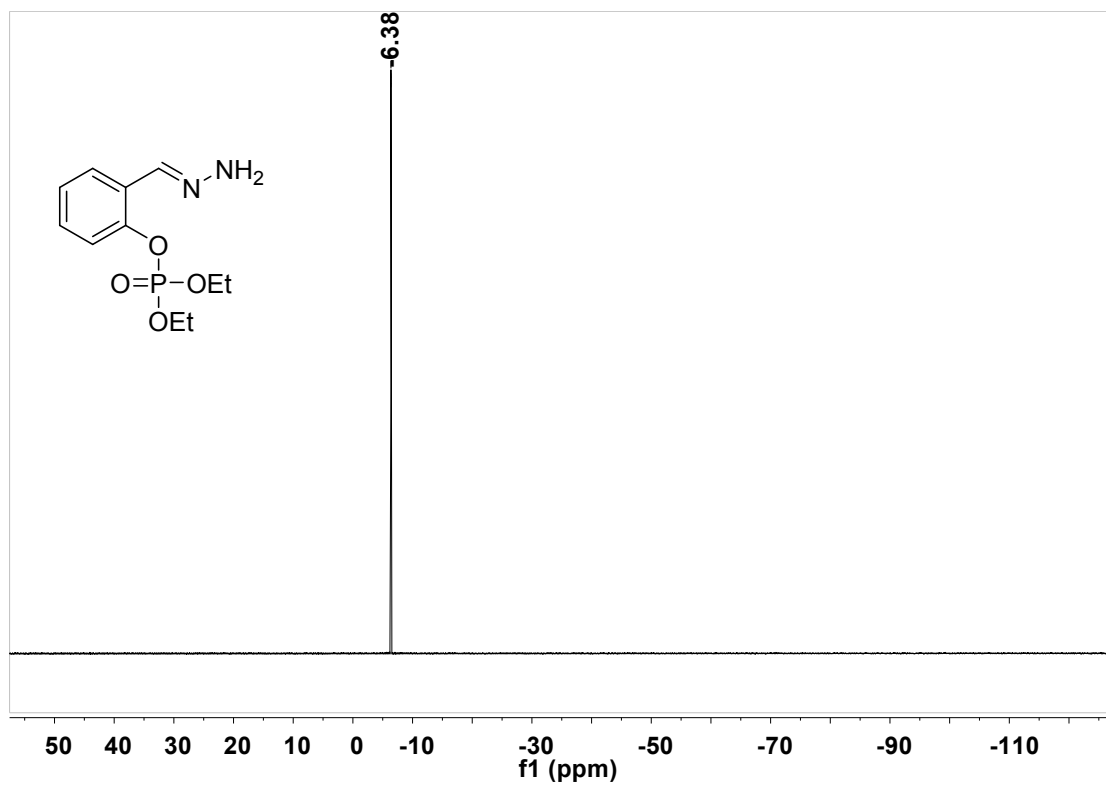


Fig. S12 ³¹P NMR spectrum of compound S-NH₂-OEt (d⁶-DMSO).

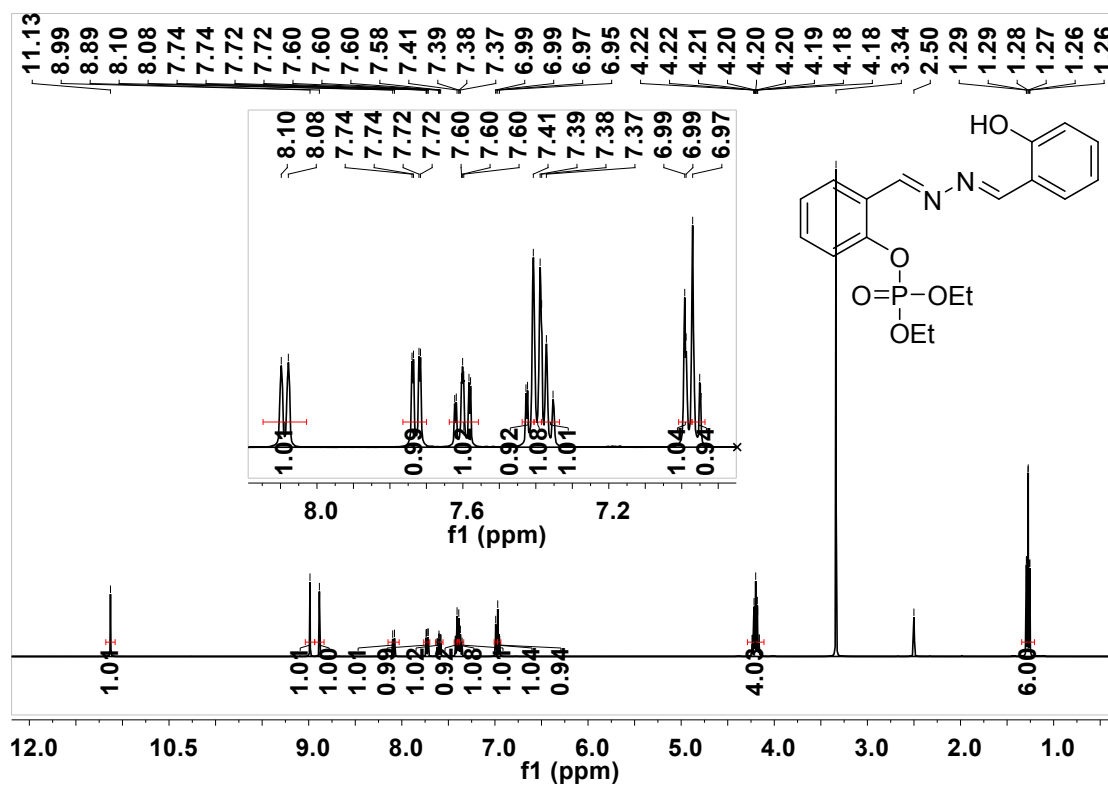


Fig. S13 ¹H NMR spectrum of compound AE-OH-OEt (d⁶-DMSO).

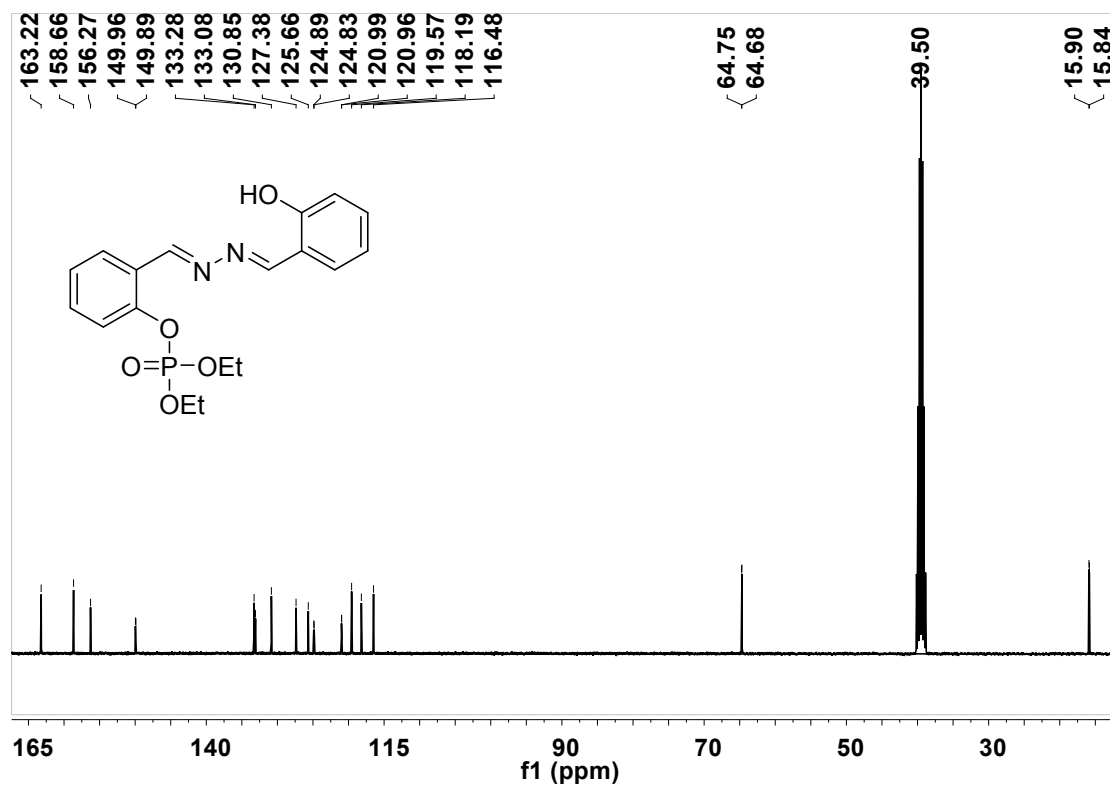


Fig. S14 ¹³C NMR spectrum of compound AE-OH-OEt (d⁶-DMSO).

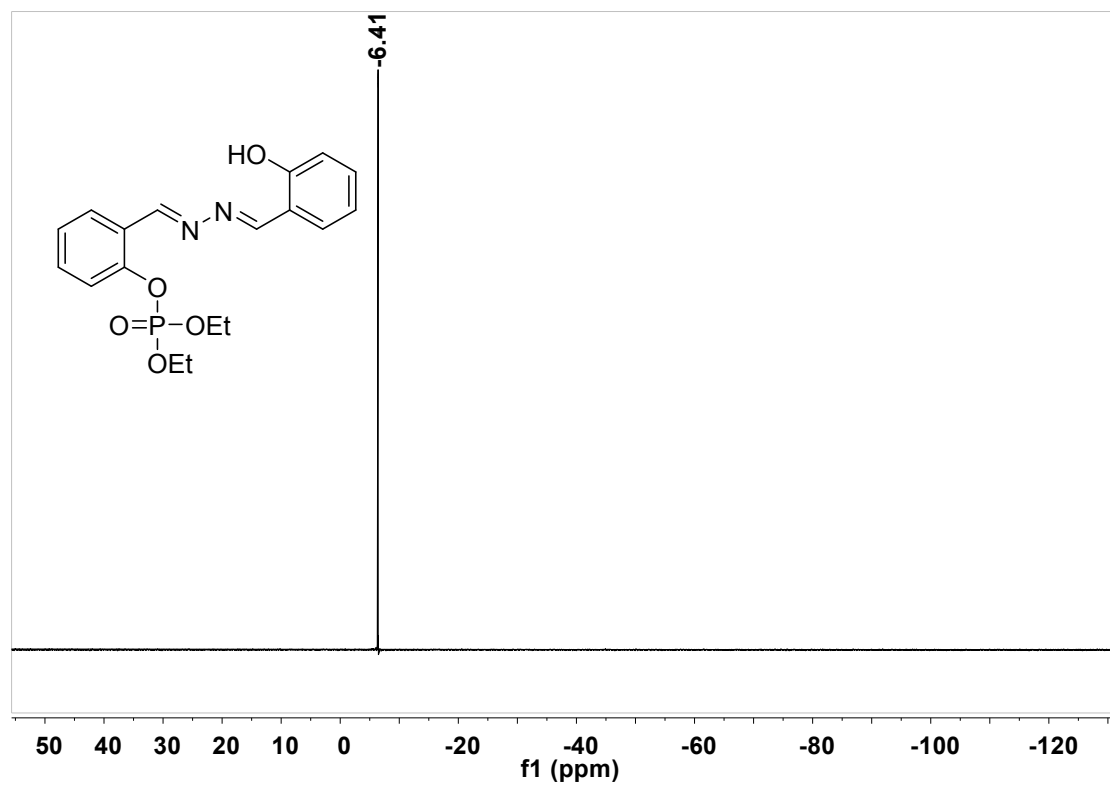


Fig. S15 ³¹P NMR spectrum of compound AE-OH-OEt (d⁶-DMSO).

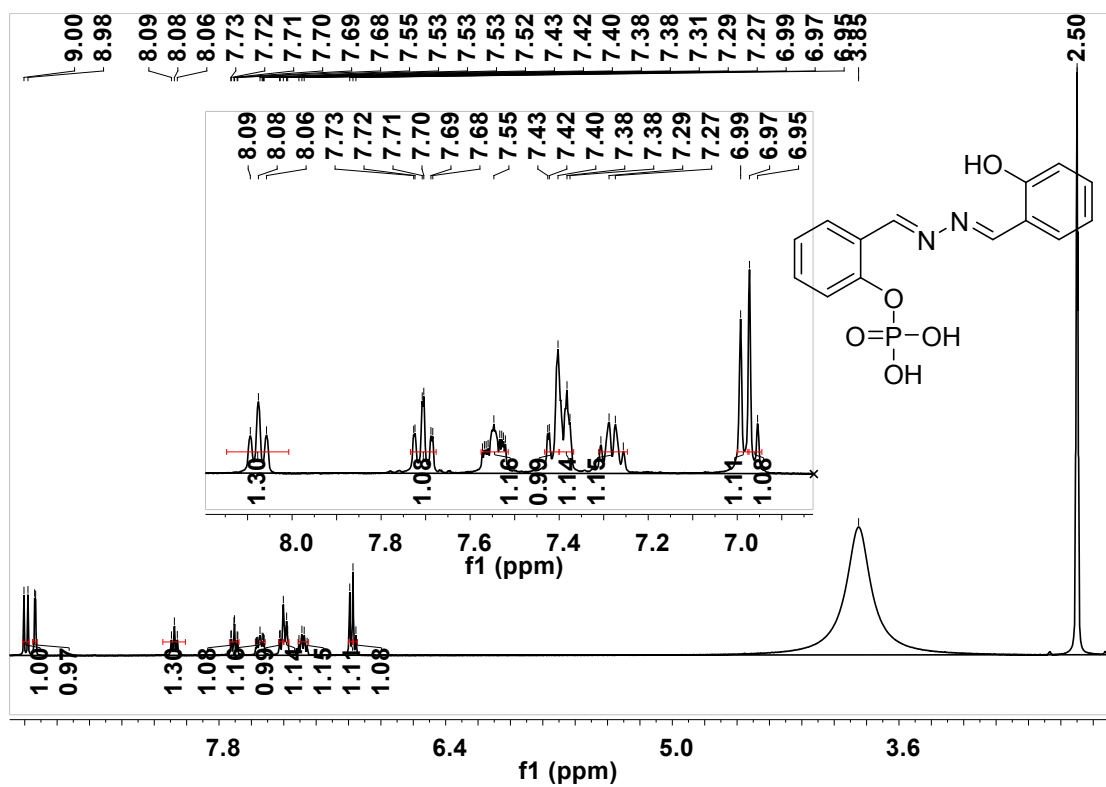


Fig. S16 ¹H NMR spectrum of compound AE-OH-Phos (d⁶-DMSO).

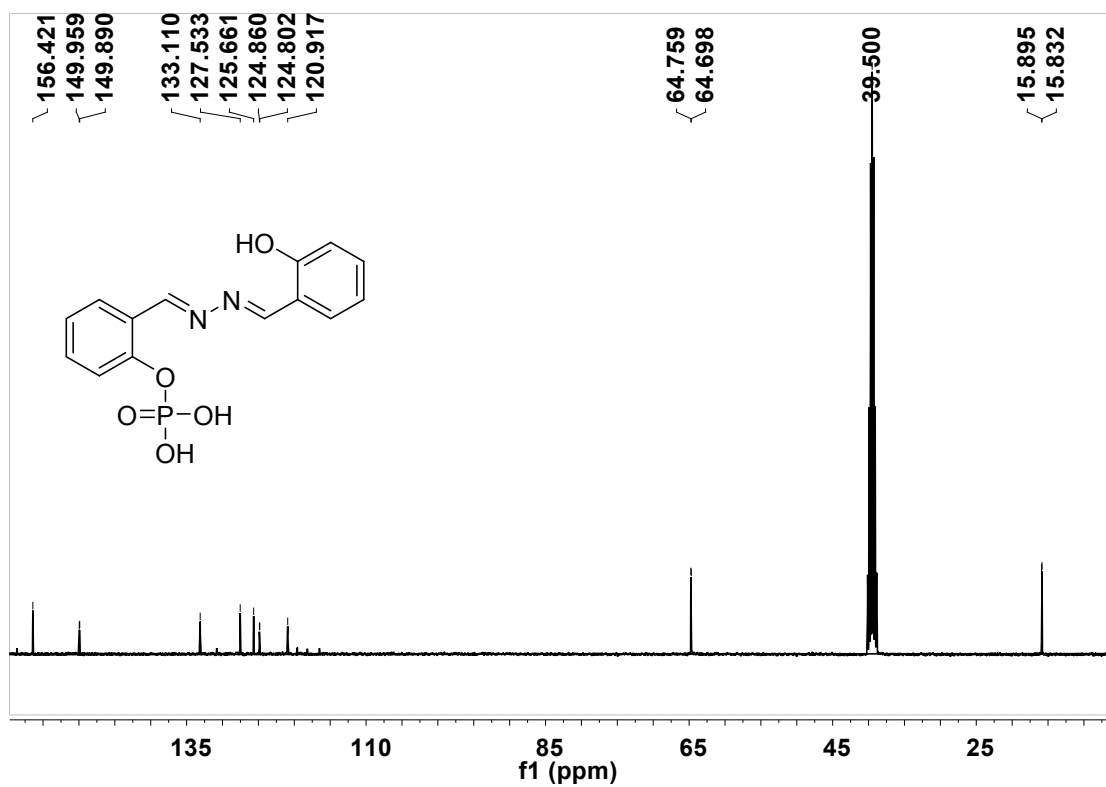


Fig. S17 ¹³C NMR spectrum of compound AE-OH-Phos (d⁶-DMSO)

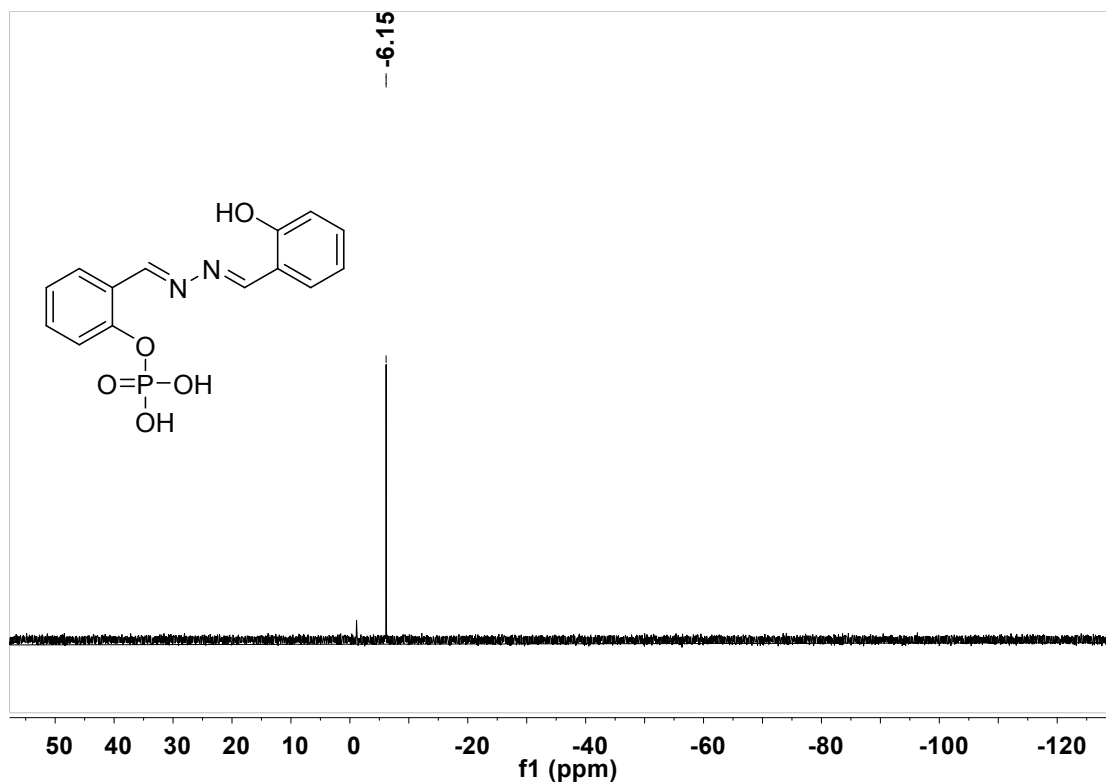


Fig. S18 ^{31}P NMR spectrum of compound AE-OH-Phos ($\text{d}^6\text{-DMSO}$).

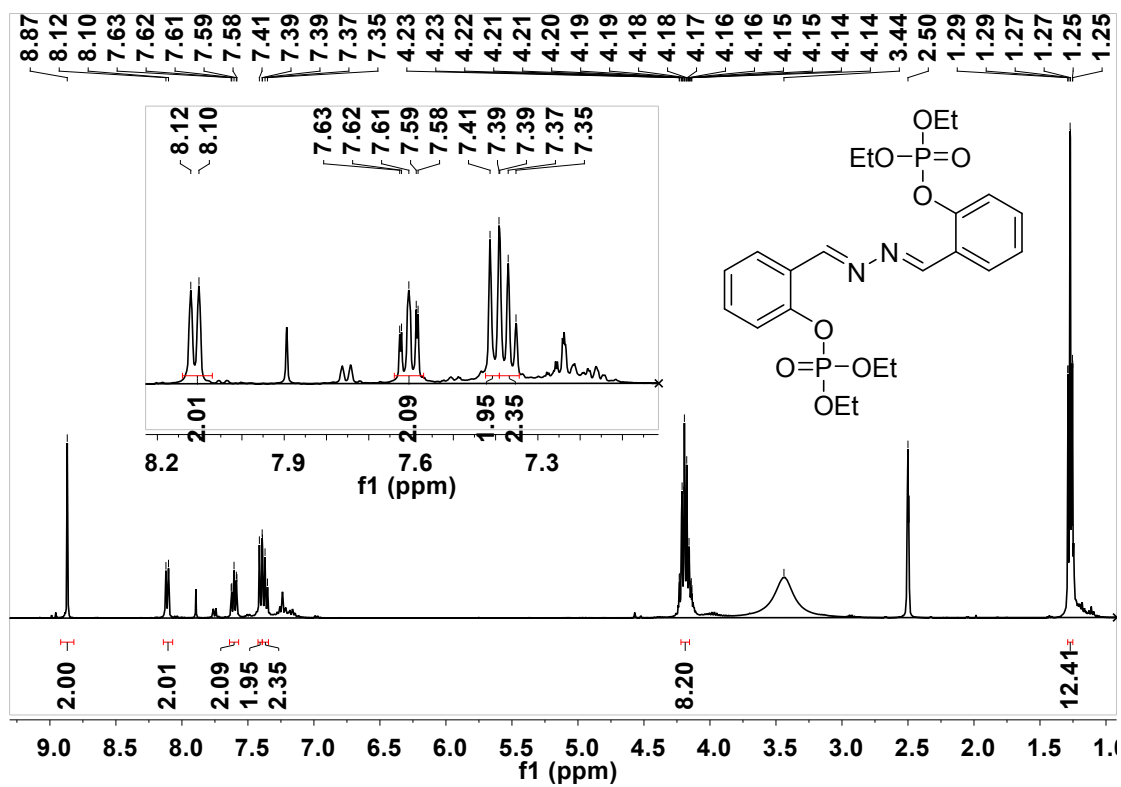


Fig. S19 ^1H NMR spectrum of compound AE-OEt ($\text{d}^6\text{-DMSO}$).

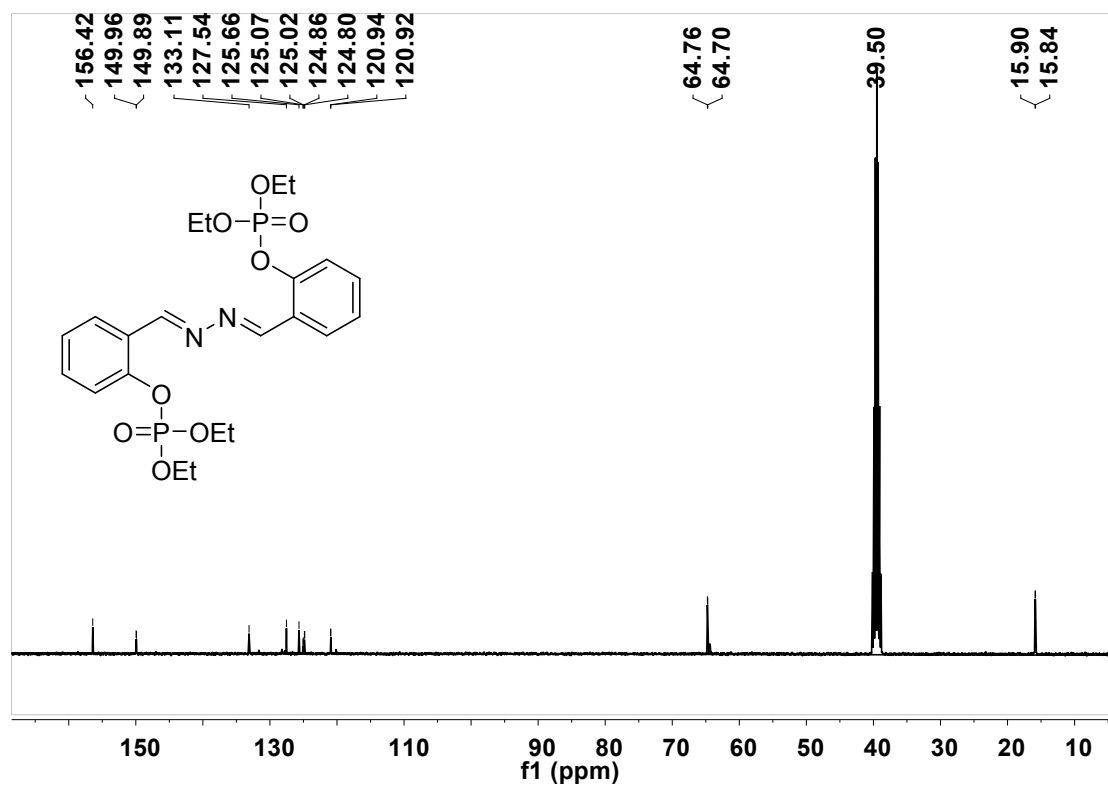


Fig. S20 ¹³C NMR spectrum of compound AE-OEt (d⁶-DMSO).

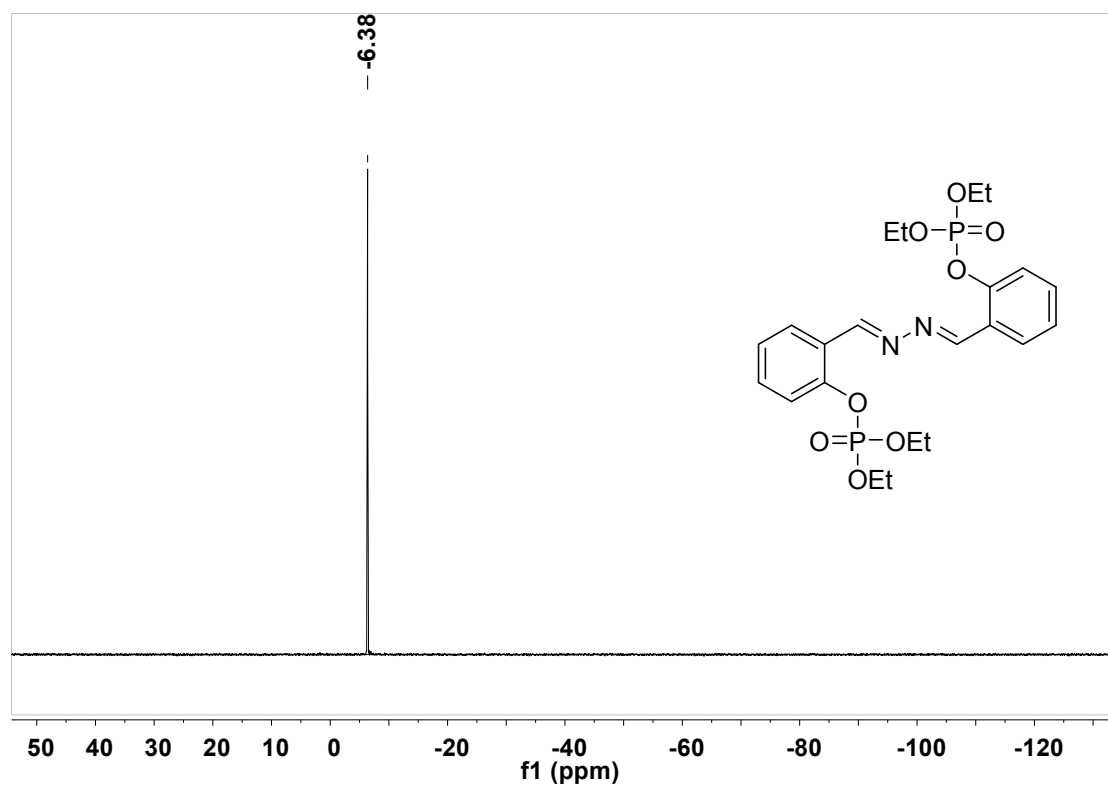
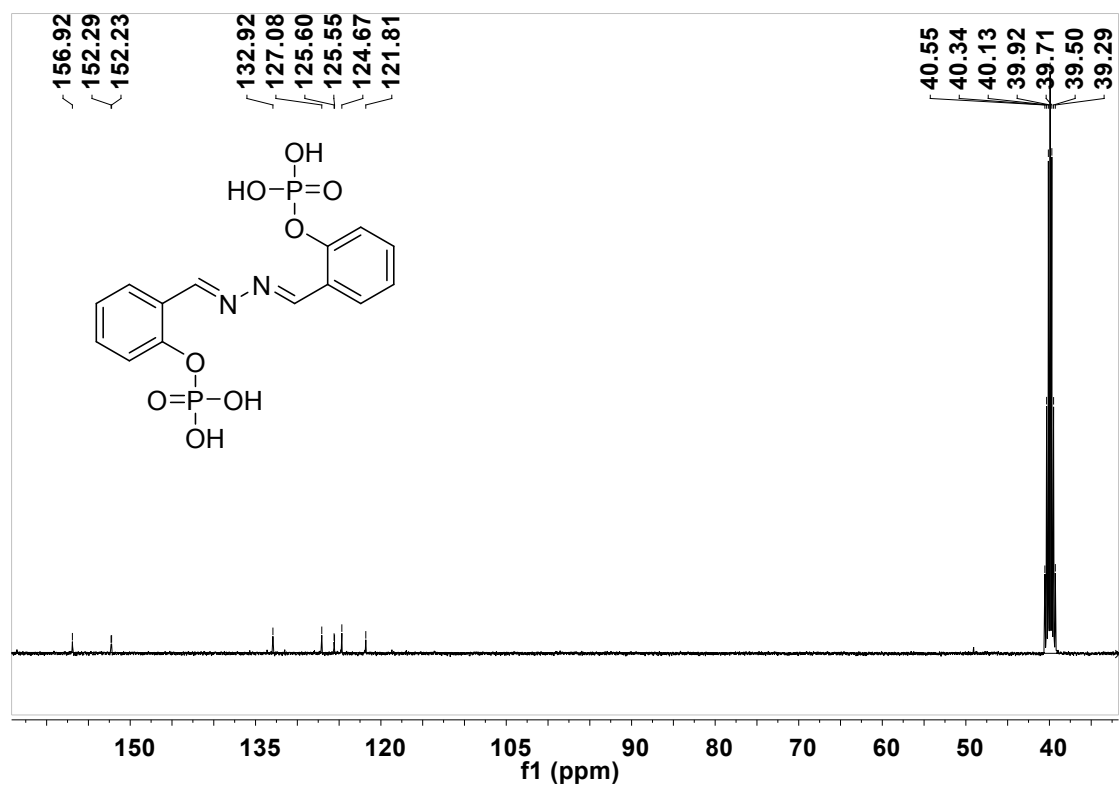
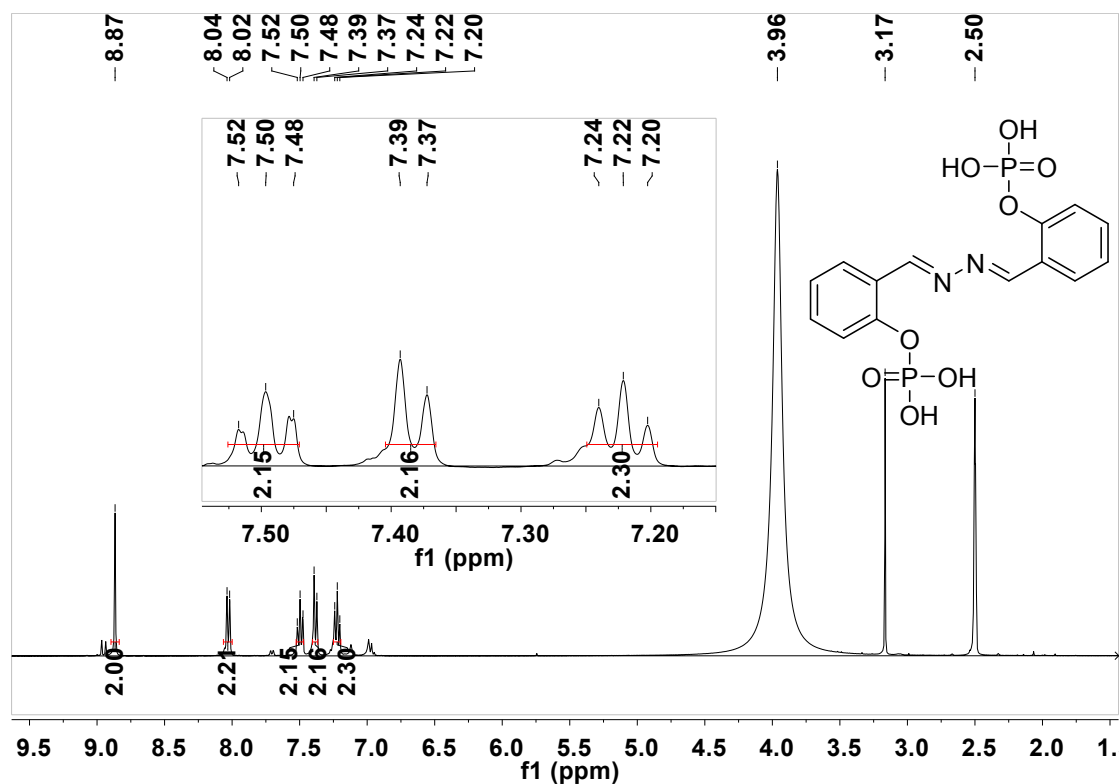


Fig. S21 ³¹P NMR spectrum of compound AE-OEt (d⁶-DMSO).



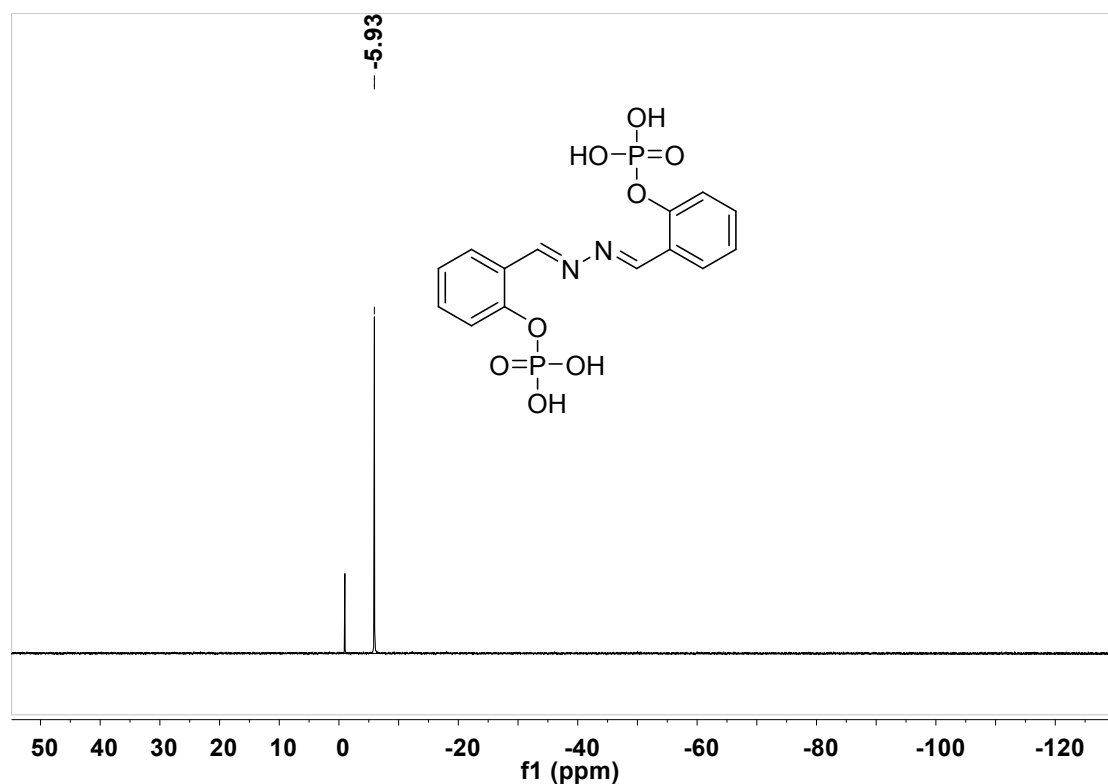


Fig. S24 ^{31}P NMR spectrum of compound AE-Phos (d^6 -DMSO).

References

- [S1] H. Zhang, P. Xiao, Y.T. Wong, W. Shen, M. Chhabra, R. Peltier, Y. Jiang, Y. He, J. He, Y. Tan, Y. Xie, D. Ho, Y.-W. Lam, J. Sun, H. Sun, Construction of an alkaline phosphatase-specific two-photon probe and its imaging application in living cells and tissues, *Biomaterials* 140 (2017) 220-229.
- [S2] Y. Tan, L. Zhang, K.H. Man, R. Peltier, G. Chen, H. Zhang, L. Zhou, F. Wang, D. Ho, S.Q. Yao, Y. Hu, H. Sun, Reaction-Based Off-On Near-infrared Fluorescent Probe for Imaging Alkaline Phosphatase Activity in Living Cells and Mice, *ACS Applied Materials & Interfaces* 9 (2017) 6796-6803.
- [S3] R. Yan, Y. Hu, F. Liu, S. Wei, D. Fang, A.J. Shuhendler, H. Liu, H.-Y. Chen, D. Ye, Activatable NIR Fluorescence/MRI Bimodal Probes for in Vivo Imaging by Enzyme-Mediated Fluorogenic Reaction and Self-Assembly, *Journal of the American Chemical Society* 141 (2019) 10331-10341.
- [S4] X. Hou, Q. Yu, F. Zeng, J. Ye, S. Wu, A ratiometric fluorescent probe for in vivo tracking of alkaline phosphatase level variation resulting from drug-induced organ damage, *Journal of Materials Chemistry B* 3 (2015) 1042-1048.
- [S5] T.-I. Kim, H. Kim, Y. Choi, Y. Kim, A fluorescent turn-on probe for the detection of alkaline phosphatase activity in living cells, *Chemical Communications* 47 (2011) 9825-9827.
- [S6] H.-W. Liu, X.-X. Hu, L. Zhu, K. Li, Q. Rong, L. Yuan, X.-B. Zhang, W. Tan, In vivo

imaging of alkaline phosphatase in tumor-bearing mouse model by a promising near-infrared fluorescent probe, *Talanta* 175 (2017) 421-426.

[S7] L. Xu, X. He, P. Ma, X. Liu, F. Zhang, Y. Sun, D. Song, X. Wang, A water-soluble fluorescent probe for the sensitive detection of endogenous alkaline phosphatase in living cells, *Dyes and Pigments* 159 (2018) 584-589.

[S8] S.-J. Li, C.-Y. Li, Y.-F. Li, J. Fei, P. Wu, B. Yang, J. Ou-Yang, S.-X. Nie, Facile and Sensitive Near-Infrared Fluorescence Probe for the Detection of Endogenous Alkaline Phosphatase Activity In Vivo, *Analytical chemistry* 89 (2017) 6854-6860.

[S9] Z. Gao, J. Sun, M. Gao, F. Yu, L. Chen, Q. Chen, A unique off-on near-infrared cyanine-based probe for imaging of endogenous alkaline phosphatase activity in cells and in vivo, *Sensors and Actuators B: Chemical* 265 (2018) 565-574.

[S10] X. Zhang, X. Chen, K. Liu, Y. Zhang, G. Gao, X. Huang, S. Hou, Near-infrared ratiometric probe with a self-immolative spacer for rapid and sensitive detection of alkaline phosphatase activity and imaging in vivo, *Analytica Chimica Acta* 1094 (2020) 113-121.